

# A versatile framework for attitude tuning of beamlines at advanced light sources

Peng-Cheng Li<sup>1,2,3,\*</sup>, Xiao-Xue Bi<sup>2,\*</sup>, Zhen Zhang<sup>1,3</sup>, Xiao-Bao Deng<sup>2</sup>,  
Chun Li<sup>2</sup>, Li-Wen Wang<sup>2</sup>, Gong-Fa Liu<sup>1,3</sup>, Yi Zhang<sup>2,3</sup>, Ai-Yu Zhou<sup>2</sup>, Yu Liu<sup>2,†</sup>

## Synopsis

Keywords: beam focusing, sample alignment, *Mamba*, virtual beamline, software architecture.

A versatile *Mamba*-based software framework for automated attitude tuning of beamlines is reported, which in our assessment is able to cover a majority of attitude-tuning (beam focusing, sample alignment *etc.*) needs in a simple and maintainable way. Apart from a few real-world examples at HEPS and BSRF, also presented is a virtual-beamline mechanism based on easily customisable simulated detectors and motors.

## Abstract

Aside from regular beamline experiments at light sources, the preparation steps before these experiments are also worth systematic consideration in terms of automation; a representative category in these steps is attitude tuning, which typically appears in names like beam focusing, sample alignment *etc.* With the goal of saving time and manpower in both writing and using in mind, a *Mamba*-based attitude-tuning framework is created. It supports flexible input/output ports, easy integration of diverse evaluation functions, and free selection of optimisation algorithms; with the help from *Mamba*'s infrastructure, machine learning (ML) and artificial intelligence (AI) technologies can also be readily integrated. The tuning of a polycapillary lens and of an X-ray emission spectrometer are given as examples for the general use of this framework, featuring powerful command-line interfaces (CLIs) and friendly graphical user interfaces (GUIs) that allow comfortable human-in-the-loop control. The tuning of a Raman spectrometer demonstrates more specialised use of the framework with customised optimisation algorithms. With similar applications in mind, our framework is estimated to be capable of fulfilling a majority of attitude-tuning needs. Also reported is a virtual-beamline mechanism based on easily customisable simulated detectors and motors, which facilitates both testing for developers and training for users.

## 1 Introduction

In beamline experiments, apart from the main scan steps (“counting”, step scans or fly scans, also including their data processing), the preparation steps before them can also be of considerable complexity, and therefore be of particular interest in terms of automation. A representative category in these steps is beam focusing (Nash et al., 2022; Takeo et al., 2020; Hong et al., 2021; Xi et al., 2017) and sample alignment (Robertson et al., 2015; Zhang et al., 2023) *etc.* At HEPS, the High Energy Photon Source (Xu et al., 2023) and BSRF, the Beijing Synchrotron Radiation Facility, we refer to these work as *attitude tuning*, borrowing the term “attitude” from aerospace

\* Li and Bi contributed equally to this paper.

† Correspondence e-mail: liuyu91@ihep.ac.cn.

<sup>1</sup> National Synchrotron Radiation Laboratory, University of Science and Technology of China, Hefei, Anhui 230029, People’s Republic of China.

<sup>2</sup> Institute of High Energy Physics, Chinese Academy of Sciences, Beijing 100049, People’s Republic of China.

<sup>3</sup> University of Chinese Academy of Sciences, Beijing 100049, People’s Republic of China.

engineering (the term “configuration” could also be considered, but would be very ambiguous). In our eyes, the essence of attitude tuning is the optimisation of certain objective parameter(s) by manual or automated tuning of the corresponding attitude parameters: *eg.* the automatic focusing of cameras is the automatic optimisation of some image definition functions by tuning parameters like focal lengths. From the information we have collected from BSRF, HEPS and our colleagues’ visits to other facilities, we find attitude tuning a ubiquitous requirement at these facilities; but given the background above, we also find that despite the diversity of devices involved in these requirements, a majority of them are fairly simple peak finding, albeit often in >1D configuration spaces.

As HEPS and other advanced light sources have small light spots and high brightness, traditional scan-based methods for attitude tuning could not only waste a lot of time (especially in >1D tuning applications), but also potentially result in more radiation damages to samples. Also considering that attitude-tuning requirements need to be implemented for the 15 beamlines in Phase I of HEPS, it is imperative for us to create an efficient and unified software framework for attitude tuning. Fortunately, *Mamba* (Liu et al., 2022; Dong et al., 2022), the *Bluesky*-based (Allan et al., 2019) software environment created for beamline experiments at HEPS, was also designed with attitude tuning and other preparation steps in mind since the very beginning. Based on it, we created a versatile framework for attitude tuning, where peak finding can be done in a simple, consistent and maintainable way. With the help from *Mamba*’s infrastructure and the rich selection of third-party Python libraries, more complex tuning, including those that require machine learning (ML) and/or artificial intelligence (AI) technologies (Rebuffi et al., 2023; Zhang et al., 2024), can also be implemented. The code for our framework is available as a part of the open-source edition of *Mamba* at <https://codeberg.org/CasperVector/mamba-ose>.

## 2 Architecture of the attitude-tuning framework

As has been noted in Section 1, we treat attitude tuning as a matter of numerical optimisation; therefore the architecture of a general-purpose attitude-tuning framework (Figure 1) will inevitably include some attitude parameters, some objective parameter(s), and some optimisation algorithm. Moreover, since the objective parameter(s) are actually obtained by physical measurement instead of purely mathematical computation, the architecture also needs to include detectors, motors and evaluation functions which convert raw data from detectors into objective values. Given these architectural elements, we implemented the `AttiOptim` class which cooperates with *Bluesky*’s interfaces for motors and detectors, as well as optimisation libraries like `scipy.optimize`. The functions `get_x()`, `put_x()` and `get_y()` in this class deal with motors and detectors by interacting with their *Bluesky* encapsulations. The function `wrap()` combines specified processing/evaluation functions with `put_x()` and `get_y()` into functions with a seemingly purely mathematical signature, which are wanted by libraries like `scipy.optimize` (*cf.* Figure 2).

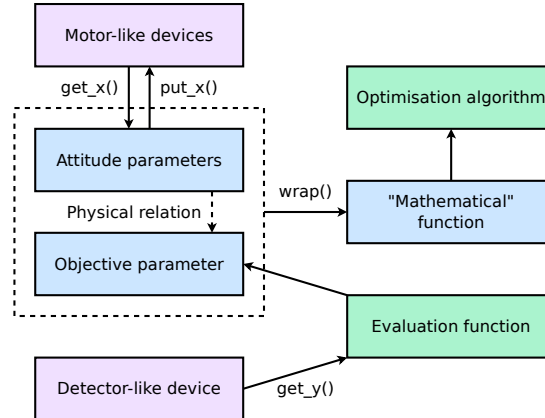


Figure 1: Architecture of our attitude-tuning framework based on `AttiOptim`.

In Section 3, we will see real-world application of our framework, using `AttiOptim`, on a polycapillary lens and an X-ray emission spectrometer: the former is more general, with a straightforward processing/evaluation function; the latter is more specialised, and demonstrates the use of a much more complex evaluation function. Then in Section 4, we will see even more specialised application of our framework on a Raman spectrometer, where the “optimisation algorithm” interface (*cf.* also Section 5) is “abused” to do parallelised peak finding of multiple objective parameters, as well as some task that is even not numerical optimisation at all. By customising `get_x()`, `put_x()` and `get_y()`, it is also possible to manipulate general motor-like devices, and possible to achieve effects like using the results from some kind of scan (*eg.* tomography or ptychography, *cf.* Zhang et al., 2023) as the raw data  $y$  for each position  $x$ , where the objective value  $z$  is computed from. With the help from *Mamba*’s infrastructure, ML/AI technologies can also be easily integrated in the evaluation function and/or the optimisation algorithm. On a deeper level, following Hutter (2020)’s treatment of AI as a matter of information compression, the pursuit of minimalist solutions for problems throughout our work in beamline control and in experiment software (Li et al., 2024) may be also seen as, in essence, a pursuit of *human intelligence* which may enlighten its AI counterparts in the same fields.

### 3 General attitude tuning: a polycapillary lens and an XES spectrometer

Our first example is about the polycapillary lens at the 4W1B beamline of BSRF, which has 4 motorised degrees of freedom: a pitch/tilt angle (`M.mCapiPitch`), a yaw/pan angle (`M.mCapiYaw`), a horizontal shift (`M.mCapiH`) and a vertical shift (`M.mCapiV`). Based on prior experience, they are split into 2 groups: the rotational parameters are the coarse tuning parameters, and the translational parameters are the fine tuning parameters; the former usually need to be tuned before the latter. The goodness of the lens’ attitude is determined by the readings from a Keithley 6482 picoammeter (`D.k6482`), which is connected to a photodiode temporarily placed next to the lens when attitude tuning is performed. The code used for this tuning based on our framework, `init_capi.py` and `lib_4w1b.py`, are available from the supplementary materials; the former mainly does *Bluesky* encapsulation of the devices involved, while the latter (with notable fragments and brief usage notes in Figure 2) contains the tuning logic. Online visual feedback of the tuning process can be done with our general-purpose graphical user interface (GUI) for attitude tuning, `mamba.attitude.capi_frontend` (Figure 3). A more feature-complete version of the GUI is shown in Figure 7(a), which most notably allows for the manual selection of axes (called  $x$  and  $y$  therein) for the 2D visualisation on the right pane; otherwise the GUI would automatically select the axes based on the latest data update.

Attitude tuning for the polycapillary lens at 4W1B of BSRF needs to be done roughly once per day during normal operation of the beamline. It used to be done by manual trial and error, each time costing around half an hour; with our attitude-tuning framework, the process has been greatly accelerated and simplified, costing just a few minutes each time and demanding much less manual intervention. From the information we have collected, attitude-tuning requirements structurally similar to the above are ubiquitous at HEPS, BSRF and other facilities, even if the devices and attitude parameters may differ greatly across beamlines. For these reasons, we believe our framework is general enough to handle this kind of application scenarios, saving great amounts of time and energy while only requiring very modest amounts of programming. We would also like to note that we are aware of the potential needs to tune multiple groups of attitude parameters, where not all groups are tuned according to the same objective parameter. In response, our framework is designed to be capable of *multi-objective tuning*: an example for it is given in the files `docs/init_capi.py` and `docs/lib_capi.py` from the open-source edition of *Mamba*; in the general-purpose visualisation GUI (Figure 7a), the objective parameter to visualise can be selected from the  $z$  axis menu.

Another example for our attitude-tuning framework is about a full-cylindrical von Hamos spectrometer (Guo et al., 2023) for X-ray emission spectroscopy (XES), currently used at 4W1B of BSRF; its use at the high pressure beamline (B6), the X-ray absorption spectroscopy beamline (B8) and possibly other beamlines at HEPS is also planned. Bragg reflection from the analyser

```

class AttiCapi(AttiOptim):
    maxfev, xatol, fatol = 100, 1, 1e-5

    # A straightforward processing/evaluation function.
    def proc(self, doc, det, motors):
        doc["data"]["meta"] = {"x": motors}
        doc["data"]["eval"] = -doc["data"]["det"]
        return doc["data"]["eval"]

    def tune_base(self, det, motors):
        dname = det.replace(".", "_")
        mnames = [m.replace(".", "_") for m in motors]
        options = {
            "disp": True, "maxfev": self.maxfev,
            "xatol": self.xatol, "fatol": self.fatol,
        }
        # The optimisation algorithm.
        return optimize.minimize(
            self.wrap([det], motors, lambda doc: self.proc(doc, dname, mnames)),
            self.get_x(motors), method = "nelder-mead", options = options
        )

    def tune_area(self, area = None):
        if area is None:
            self.tune_area("rot")
            self.tune_area("trans")
        elif area == "rot":
            self.tune_base("D.k6482", ["M.mCapiPitch", "M.mCapiYaw"])
        elif area == "trans":
            self.tune_base("D.k6482", ["M.mCapiH", "M.mCapiV"])
        else:
            raise RuntimeError("unknown area '%s'" % area)

    # Users simply run `U.atti_capi.tune("rot")` and `U.atti_capi.tune("trans")`
    # to tune, respectively, the rotational and translational axes.
    @stage_wrap
    def tune(self, *args, **kwargs):
        [fix_zero(m) for m in self.motors.values()]
        self.tune_area(*args, **kwargs)

```

Figure 2: Notable fragments of lib\_4w1b.py with brief usage notes.

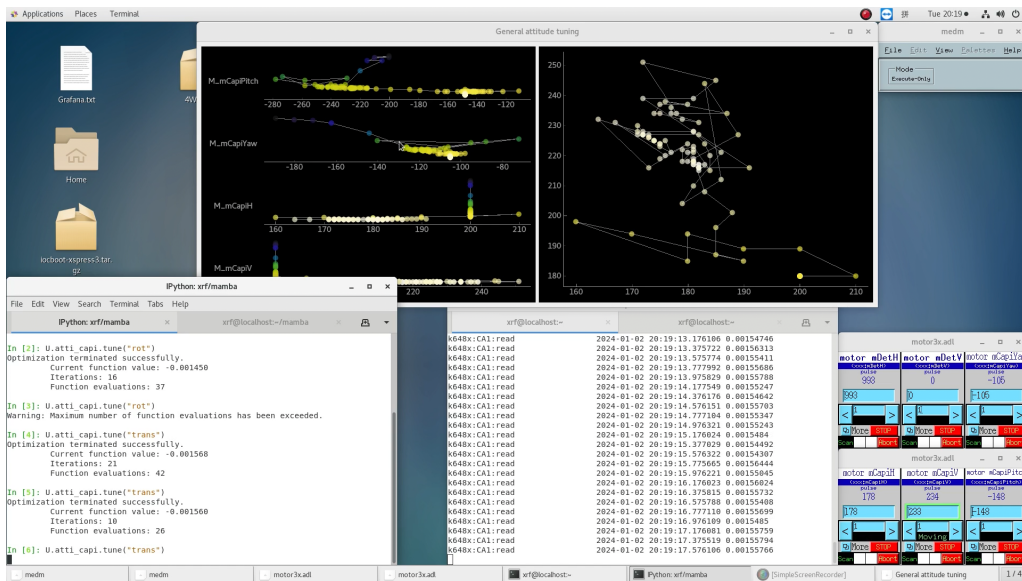


Figure 3: Attitude tuning of the polycapillary lens at 4W1B of BSRF.

of the spectrometer produces circular patterns in images acquired from the detector (Figure 4); the pitch/tilt and yaw/pan angles are tuned to optimise the shape of the circle, so that a sharpest peak is obtained on the radial distribution curve, shown on the lower pane of the main window in the figure. More precisely, the half-maximum region of interest (HM-ROI) is computed for the radial distribution, then the mean intensity in this ROI is used as the objective parameter. From the description above it can already be seen that for the tuning of this spectrometer, the processing/evaluation function needed must have a non-trivial complexity. But in addition to this, another main source of complexity is the selection of centre (origin) of the circles, where inappropriately selected origins can result in distorted peaks and unoptimal attitudes.

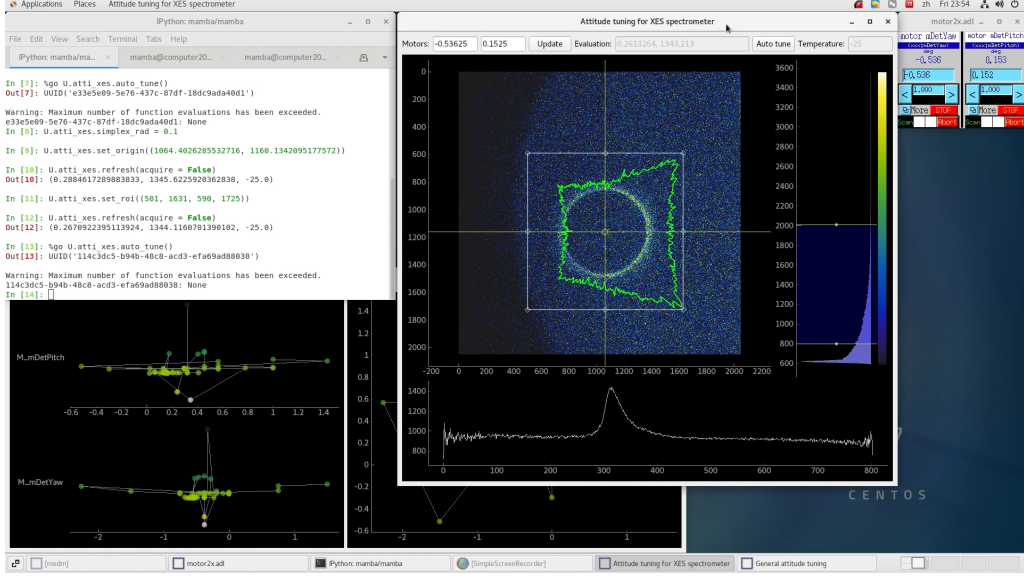


Figure 4: Attitude tuning of an XES spectrometer at 4W1B of BSRF.

Noticing that automated origin selection is a computationally expensive process which however only needs to be done after significant changes to the attitude, we decided to use a *human-in-the-loop* approach for it. An “Auto origin” button is provided in the GUI (*cf.* the more feature-complete version in Figure 7a) for automated fine tuning of the origin, whose coarse selection can be done manually by dragging the origin point shown in the GUI. In the light of the analyses above, we wrote the specialised attitude-tuning program for this XES spectrometer as `mamba.attitude.xes_backend` and `mamba.attitude.xes_frontend`, where the latter is the main GUI shown in the figures above. Considering that radial distributions and raw images are the main data wanted by users in normal data acquisition (“counting”) after attitude tuning has been done, this program is also written with normal counting in mind: the GUI provides features wanted by users, like setting acquisition time and saving experiment data. As attitude tuning is normally done by beamline staffs, and the tuning process (except for origin selection) is already convenient enough for them on the command line, there is no GUI button for it. Other than the general-purpose `mamba.attitude.capi_frontend` (as is with the polycapillary lens above), visualisations in the specialised GUI will also be automatically updated after each move in the tuning process.

## 4 Specialised attitude tuning: an XRS spectrometer

Among the instruments at the hard X-ray high-resolution spectroscopy beamline (B5) of HEPS, currently under active construction, is an X-ray Raman scattering (XRS) spectrometer. Structurally similar to the spectrometer in (Huotari et al., 2017), the XRS spectrometer at B5 of HEPS has 6 analyser modules, each containing one detector and a  $3 \times 5$  array of analysers; each analyser has three motorised degrees of freedom – one longitudinal shift and two latitudinal angles. As is shown in Figure 5, latitudinal tuning ( $x_1$  and  $x_2$  for each analyser) moves the X-ray spots around on detectors, while longitudinal tuning ( $x_0$  for each analyser) focuses the spots. After the spots are

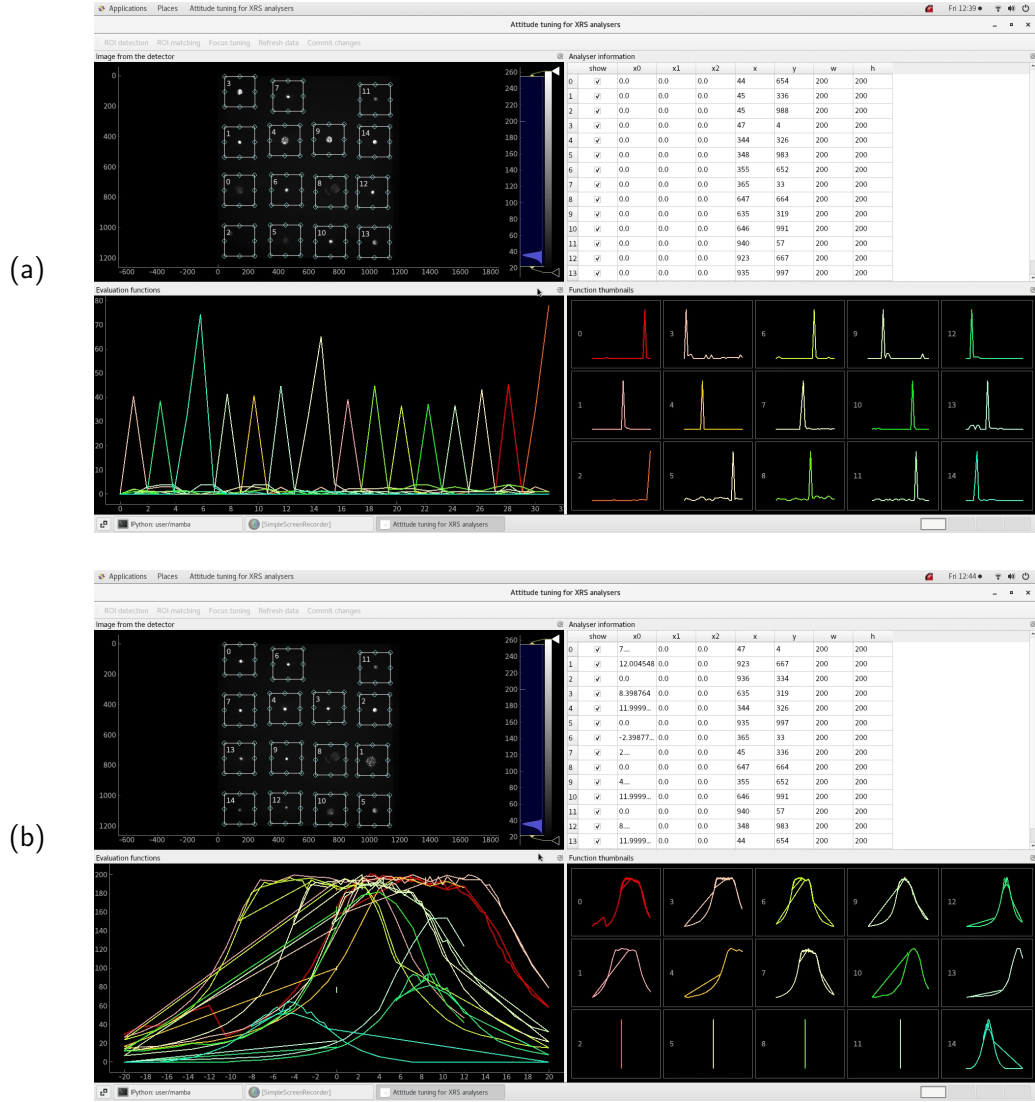


Figure 5: GUI of our XRS attitude-tuning program, doing (a) ROI matching and (b) focus tuning; the pictures are obtained from a laser-based simulation of what would eventually be done with X-ray at HEPS. Motor motion and ROI editing can be done on the top-right pane; ROIs can also be modified with mouse operations on ROI rectangles on the top-left pane, and/or with drag-and-drop operations of table rows on the top-right pane. Automated tuning is currently only implemented for a single analyser module, while parallelised tuning of multiple modules will be implemented in the future.

properly distributed and each of them is correctly assigned to the corresponding analyser, focus tuning is performed; all these steps can be done in the GUI of our specialised attitude-tuning program for this spectrometer, `mamba.attitude.raman_backend` and `mamba.attitude.raman_frontend`. Spot distribution is done manually with visual aid from the GUI, spot assignment (ROI detection followed by ROI matching) is automated, while focus tuning is automated and parallelised. Due to the use of multiplexers for motion controllers (Li et al., 2024), the motors in each analyser module are separated into multiple groups, where two motors in the same group cannot be moved at the same time. Consequently, in our program the parallelisation of focus tuning is done in multiple passes: the first motor in every longitudinal group, then the second, *etc.*

Focus tuning of the XRS spectrometer at B5 of HEPS is based on a 2D generalisation of the HM-ROI mean in Section 3 as the objective parameter. Other than application on spectrometers in this paper, similar evaluation functions have also been used in a few other scenarios, *eg.* the standalone X-ray beam position monitor (XBPM) program in (Li et al., 2024) based on images from area detectors. The optimisation is implemented by multiple calls to `max_parascan()`, a function that optimises, in parallel, the objective parameter for each ROI in the list of ROIs passed to this function. This function’s signature is similar to *eg.* `scipy.optimize.minimize()`, except that its objective function produces an 1D numerical array instead of a 0D number. Internally, it first does a coarse inner-product scan (*cf.* `scan()` from *Bluesky*) for elements of the input parameter, then does a fine inner-product scan of the input elements in the reverse direction, and finally sets the input elements to the peak positions (*cf.* Figure 8 for the details). ROI matching is implemented with `perm_diffmax()`, a function with a signature similar to `max_parascan()`; its “objective function” computes all X-ray spots’ barycentres inside their HM-ROIs (which are also used in the XBPM program mentioned above), as well the distance from each barycentre to a corresponding reference position. For each analyser, `perm_diffmax()` sets the reference positions to the initial positions of the barycentres; it then changes the latitudinal parameters of this analyser in small steps until a spot/ROI stands out with a significantly larger distance than those of all the rest. This outstanding ROI is assigned to the current analyser, and the latitudinal parameters are reset to the original values; the reference positions are updated to counteract potential motor backlashes, and then `perm_diffmax()` moves on to the next analyser. `perm_diffmax()` finally returns the mapping table from ROIs to analysers, which is applied in the command-line backend and GUI frontend of our program.

```
import numpy
from ophyd import EpicsMotor
from butils.sim import SimMotorImage
def rosenbrock(x):
    return (100.0 * (x[1:] - x[:-1] ** 2.0) ** 2.0 + (1 - x[:-1]) ** 2.0).sum(0)
def test_obj(x):
    return rosenbrock(x) + numpy.random.normal(scale = 1e-2, size = x.shape[1:])
class MySimImage(SimMotorImage):
    def bind(self, obj, motors):
        self.obj, self.motors = obj, motors
        return self.mbind(motors)
    def func(self):
        return self.obj(numpy.array([m.position for m in self.motors]))
m1, m2, m3 = [EpicsMotor("IOC:" + k, name = "M." + k)
               for k in ["m1", "m2", "m3"]]
rosen = MySimImage(name = "rosen")
rosen.bind(test_obj, [m1, m2, m3])
```

Figure 6: A virtual device connected to 3 *motorMotorSim*-based motors, based on the Rosenbrock function widely used to test optimisation algorithms, perturbed by a random noise.

In the end of this section, we briefly introduce the virtual-beamline mechanism which we now use extensively both in attitude tuning and in other applications. First, based on the *motorMotorSim* and *ADSimDetector* modules in *EPICS*, we are already able to perform many kinds of simulations, also including those independent of *Bluesky*, *eg.* the Python IOC for motor multiplexers in (Li et al., 2024). We note that the former is especially useful because of its realistic simulation of motor speeds, soft limits *etc.* Second, we also created the `butils.sim` module for *Mamba*, which



provides useful and easy-to-use simulation device classes that expose interfaces similar to those of *Bluesky*'s classes for real devices. For example, the `SimMotorImage` class (Figure 6) implements a virtual device that binds to a simulation function and some motor-like device object(s), whether real motors, simulated motors like those based on `motorMotorSim`, or even things like energies of monochromators; it produces readings according to the device positions and the simulation function. Based on the mechanisms above, we are able to create virtual beamlines to test programs and train staffs/users, saving lots of beamtime and allowing for the development of software before the required instruments are fully ready. For instance, with virtual beamlines we can test our attitude-tuning programs (Figure 7; all the simulation code is available in the `docs` subdirectory of the open-source edition of *Mamba*) extensively before their tests on real hardware, and often only need minor tweaks/fixes in the latter tests.

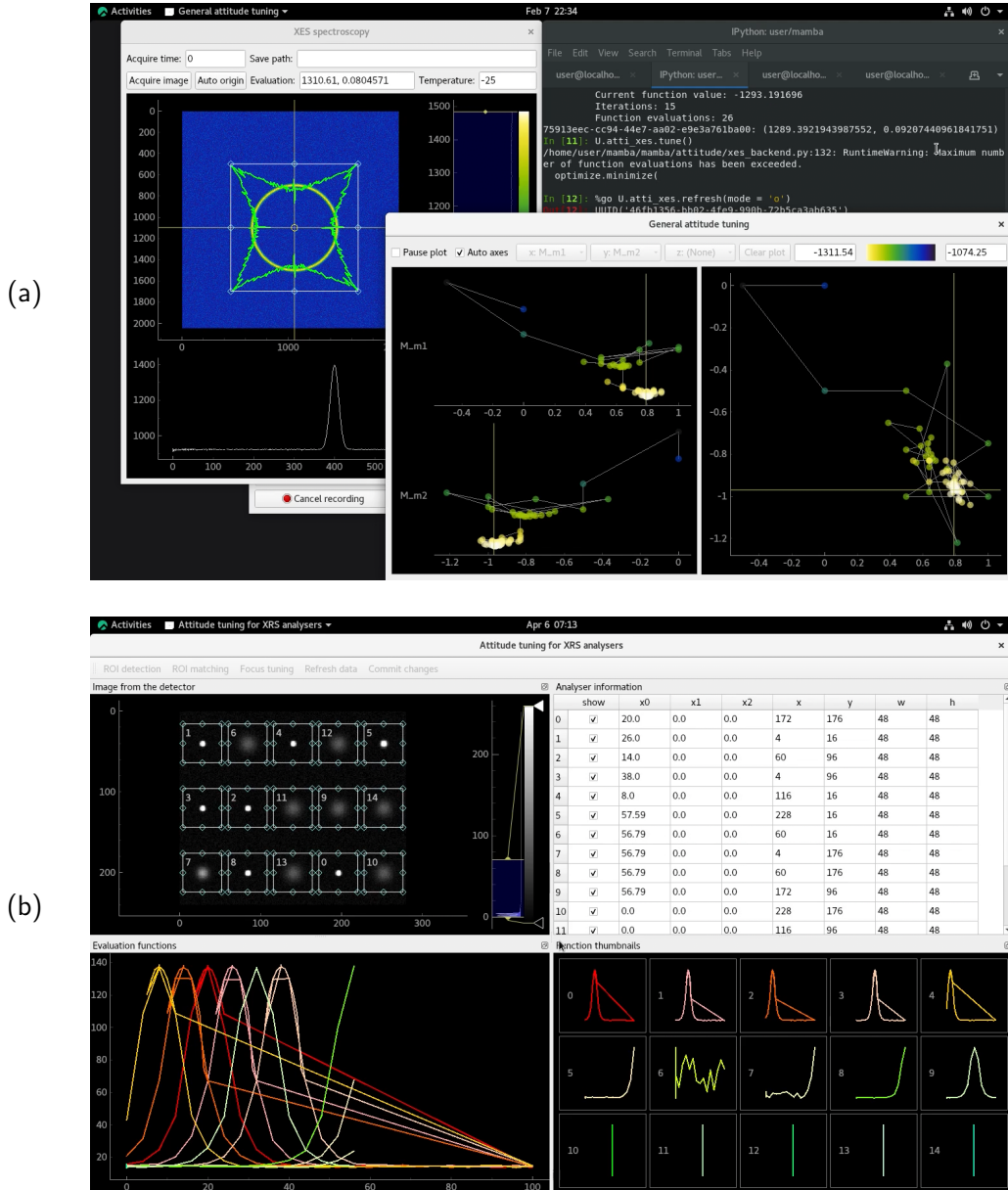


Figure 7: Our (a) XES and (b) XRS attitude-tuning programs running with virtual beamlines.



## 5 Outlook and discussion

With the real-world examples in Sections 3–4, and noticing the architectural versatility of our attitude-tuning framework (*cf.* Section 2), we believe this framework is able to cover a majority of attitude-tuning needs in a simple and maintainable way, especially during the normal operation of facilities/beamlines. On the other hand, we are also exploring the use of our framework during the construction phase of facilities/beamlines, where the relations between attitude parameters and objective parameters would often be much more complicated. We are also aware of requirements outside of beamlines that structurally resemble attitude tuning, *eg.* the tuning of beams in accelerators (Emery et al., 2021) and the calibration of detectors (*cf.* the *xspress3-autocalib* program for the Xspress3 readout system for silicon drift detectors and high-purity germanium detectors); collaboration toward these directions have also been envisioned.

In the rest of this section, we would like to discuss a few issues we find with current numerical optimisation libraries during their application in attitude tuning. These issues originate from physical factors that are typically less considered in the field of numerical optimisation, and we hope the following discussions can raise mathematicians’ awareness of them. A first of them is about the serial nature of numerical optimisation in attitude tuning: except for tuning of simulations (*eg.* digital twins) of physical systems, the tuning is based on manipulation of motor-like devices and readings from detectors, which are in general not susceptible to parallelisation. Mathematically, this makes parallel optimisation algorithms (genetic algorithms, particle swarm optimisation *etc.*) unsuitable for attitude tuning. Furthermore, as the efficiency of attitude tuning often depends not only on the number of optimisation moves, but also the trajectory length due to the movement of motors, optimisation algorithms that aim on shortening the trajectory may be a research direction worthy of systematic consideration. We additionally note that fly scans may be worth special attention in this research direction, since they can quickly sample large numbers of points on the motion trajectories.

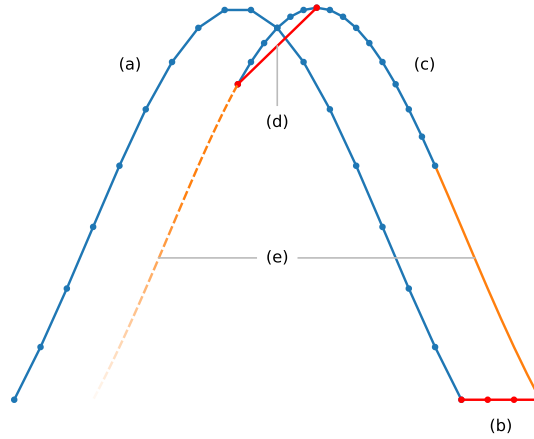


Figure 8: Objective parameter curve of the `max_parascan()` algorithm for each motor, where dots indicate scan points: (a) normal part of the coarse scan; (b) part of the coarse scan that may appear when the motor is stalled by a stopper; (c) the fine scan, which starts at the rightmost point where the objective value rose above a first threshold in the coarse scan, and stops when the objective value falls below a second threshold; (d) the final move to the peak position, deemed by the algorithm as the centre of the interval in the fine scan where the objective values were above the second threshold above; (e) intervals skipped by the fine scan to save time.

Another issue we find is the precision limits in manipulation and measurement of physical systems, *eg.* the step sizes of stepping motors; they can lead to pathological behaviours in some algorithms on certain conditions, which require workarounds like `fix_zero()` in the file `lib_4w1b.py` (*cf.* Section 3). On a deeper level, this is because of the assumption in optimisation algorithms that the readback values of position  $x$  were always equal to the setpoints; similarly, most optimisation algorithms do not consider possible measurement errors in the objective value  $z$ , except

for *eg.* those in the *Noisyopt* library (Mayer, 2016). In comparison with the minor noises in attitude parameters and objective parameters that stem from precision limits and measurement errors, hysteresis-like effects (*eg.* motor backlashes) and drifting of physical systems (*eg.* beam orbit drifting in accelerators) can result in bigger troubles, and may require special treatments in the optimisation algorithms used. For instance, because of multiple engineering reasons, the XRS spectrometer in Section 4 has no limit switches or motor encoders, and instead only has stopper blocks at the boundaries; so after a focusing motor gets stalled by a stopper, the effect in Figure 8(b) will be observed on the objective parameter. Consequently, the `max_parascan()` algorithm in Section 4 was designed with resistance against this effect in mind, and the resistance can be tuned with its threshold parameters.

## 6 Conclusion

The preparation steps in beamline experiments can also be of particular interest in terms of automation, and a representative category in these steps is attitude tuning, including beam focusing, sample alignment *etc.* We find attitude tuning a ubiquitous requirement at light sources, and a majority of these requirements are fairly simple peak finding. Noticing the nature of advanced light sources and the complexity of requirements at new light sources at HEPS, we created a versatile framework for attitude tuning based on *Mamba*. We treat attitude tuning as a matter of numerical optimisation, so based on the elements in numerical optimisation and physical measurement, we implemented the `AttiOptim` class which cooperates with *Bluesky*’s interfaces for motors and detectors, as well as optimisation libraries like `scipy.optimize`. Aside from regular peak finding, by customising `AttiOptim` it is also possible to manipulate general motor-like devices, and possible to achieve effects like using the results from some kind of scan as the raw data for each position. With the help from *Mamba*’s infrastructure, ML/AI technologies can also be easily integrated in our attitude tuning framework.

The first real-world example for our framework is the attitude tuning of the polycapillary lens at 4W1B of BSRF, which demonstrates how to do simple peak finding with straightforward processing/evaluation functions; structurally similar attitude-tuning requirements are ubiquitous at light sources. Also introduced with this example is a general-purpose visualisation GUI for attitude tuning, and the support for multi-objective tuning in our framework. The next example is the tuning of a von Hamos XES spectrometer at 4W1B of BSRF, which uses a much more complex evaluation function; it also shows a way human-in-the-loop control can be integrated in attitude tuning, where the human inputs are reused in normal “counting” after the tuning. The final example is the tuning of the XRS spectrometer at B5 of HEPS, where the “optimisation algorithm” interface is “abused” to do parallelised peak finding of multiple objective parameters, as well as the automated assignment of X-ray spots to analysers which is not numerical optimisation at all.

With these examples, and noticing the architectural versatility of our framework, we believe it is able to cover a majority of attitude-tuning needs in a simple and maintainable way. Also reported is a virtual-beamline mechanism based on easily customisable simulated detectors and motors, which facilitates both testing for developers and training for users. We noticed a few algorithmic issues in attitude tuning, which stem from physical factors less considered in the field of numerical optimisation, and may require attention from mathematicians: the unsuitability of parallelisation; the importance of shortening the trajectory of optimisation; the relevance of fly scans; the difference between readback values and setpoints; measurement errors in objective parameters; hysteresis-like effects and drifting of physical systems.

## Acknowledgements

The authors would like to thank the B5 beamline of HEPS and the 4W1B beamline of BSRF for a large fraction of motivations for this paper. This work was supported by the National Key Research and Development Program for Young Scientists (Grant No. 2023YFA1609900) and the Young Scientists Fund of the National Natural Science Foundation of China (Grants Nos. 12205328, 12305371).

## References

- Allan, D., Caswell, T., Campbell, S. and Rakitin, M., 2019. Bluesky's ahead: A multi-facility collaboration for an a la carte software project for data acquisition and management. *Synchrotron radiat. news*, 32(3), pp.19–22.
- Dong, Y.H., Li, C., Zhang, Y., Li, P.C. and Qi, F.Z., 2022. Exascale image processing for next-generation beamlines in advanced light sources. *Nat. rev. phys.*, 4(5), pp.427–428.
- Emery, L., Shang, H.R., Sun, Y.P., and Huang, X.B., 2021. Application of a machine learning based algorithm to online optimization of the nonlinear beam dynamics of the argonne advanced photon source. *Phys. rev. accel. beams*, 24(8), p.082802.
- Guo, Z.Y., Zhang, Y.J., Xu, W., Jin, S.X., Gan, X.L., Zhang, H., Chen, D.L. and Jia, Q.J., 2023. A von hamos full-cylindrical spectrometer based on striped si/ge crystal for advanced x-ray spectroscopy. *Rev. sci. instrum.*, 94(2), p.023102.
- Hong, C.X., Zhou, P., Hua, W.Q., Yang, C.M. and Bian, F.G., 2021. Automatic calibration system of small angle x-ray scattering experiment station at ssrf. *Nuclear techniques*, 44(1), p.010102.
- Huotari, S., Sahle, C.J., Henriquet, C., Al-Zein, A., Martel, K., Simonelli, L., Verbeni, R., Gonzalez, H., Lagier, M.C., Ponchut, C., Sala, M.M., Krisch, M. and Monaco, G., 2017. A large-solid-angle x-ray raman scattering spectrometer at id20 of the european synchrotron radiation facility. *J. synchrotron rad.*, 24(2), pp.521–530.
- Hutter, M., 2020. 500'000€ prize for compressing human knowledge. Available from: <http://prize.hutter1.net/>.
- Li, P.C., Bi, X.X., Huang, Y.K., Zhang, D.S., Deng, X.B., Zhang, Q., Lei, G., Li, G. and Liu, Y., 2024. Beyond the epics: comprehensive python ioc development with queueioc. Available from: <https://arxiv.org/abs/2411.01258>.
- Liu, Y., Geng, Y.D., Bi, X.X., Li, X., Tao, Y., Cao, J.S., Dong, Y.H. and Zhang, Y., 2022. Mamba: a systematic software solution for beamline experiments at heps. *J. synchrotron rad.*, 29(3), pp.664–669.
- Mayer, A., 2016. Noisyopt: A python library for optimizing noisy functions. Available from: <https://noisyopt.readthedocs.io/en/stable/>.
- Nash, B., Abell, D., Nagler, R., Moeller, P., Keilman, M., Pogorelov, I., Goldring, N., Rakitin, M., Lynch, J., Giles, A., Walter, A., Maldonado, J., Morris, T., Bak, S. and Du, Y., 2022. Combining diagnostics, modeling, and control systems for automated alignment of the tes beamline. *J. phys.: Conf. ser.*, 2380, p.012103.
- Rebuffi, L., Kandel, S., Shi, X.B., Zhang, R.Y., Harder, R.J., Cha, W., Highland, M.J., Frith, M.G., Assoufid, L. and Cherukara, M.J., 2023. Autofocus: Ai-driven alignment of nanofocusing x-ray mirror systems. *Opt. express*, 31(24), pp.39514–39527.
- Robertson, W.D., Porto, L.R., Ip, C.J.X., Nantel, M.K.T., Tellkamp, F., Lu, Y.F. and Miller, R.J.D., 2015. Note: A simple image processing based fiducial auto-alignment method for sample registration. *Rev. sci. instrum.*, 86(8), p.086105.
- Takeo, Y., Motoyama, H., Shimamura, T., Kimura, T., Kume, T., Matsuzawa, Y., Saito, T., Imamura, Y., Miyashita, H., Hiraguri, K., Hashizume, H., Senba, Y., Kishimoto, H., Ohashi, H. and Mimura, H., 2020. A highly efficient nanofocusing system for soft x-rays. *Appl. phys. let.*, 117(15), p.151104.
- Xi, S.B., Borgna, L.S., Zheng, L.R., Du, Y.H. and Hu, T.D., 2017. Ai-bl1.0: a program for automatic on-line beamline optimization using the evolutionary algorithm. *J. synchrotron rad.*, 24(1), pp.367–373.

- Xu, H.S., Meng, C., Peng, Y.M., Tian, S.K., Wang, N., Cui, X.H., Du, C.C., Duan, Z., Guo, Y.Y., He, P., Huang, X.Y., Ji, D.H., Ji, H.F., Jiao, Y., Li, J.Y., Li, N., Li, X.Y., Lu, X.H., Liang, P.F., Pan, W.M., Qu, H.M., Wang, B., Wang, J.Q., Wei, Y.Y., Wan, J.Y., Xu, G., Yan, F., Yu, C.H., Yue, S., Zhang, X. and Zhao, Y.L., 2023. Equilibrium electron beam parameters of the high energy photon source. *Radiat. detect. technol. methods*, 7(2), pp.279–287.
- Zhang, Z., Bi, X.X., Li, P.C., Zhang, C.L., Yang, Y.M., Liu, Y., Chen, G., Dong, Y.H., Liu, G.F. and Zhang, Y., 2023. Automatic synchrotron tomographic alignment schemes based on genetic algorithms and human-in-the-loop software. *J. synchrotron rad.*, 30(1), pp.169–178.
- Zhang, Z., Li, C., Wang, W.H., Dong, Z., Liu, G.F., Dong, Y.H. and Zhang, Y., 2024. Towards full-stack deep learning-empowered data processing pipeline for synchrotron tomography experiments. *Innovation*, 5(1), p.100539.